

# DESIGN OF A MICROBUNCHED ELECTRON COOLER ENERGY RECOVERY LINAC

K. Deitrick\*, S. Benson, B.R. Gamage, J. Guo, I. Neththikumara, R. Rimmer, T. Satogata, N. Sereno, S. Setiniyaz, Thomas Jefferson National Accelerator Facility, Newport News, VA, USA  
 J. Conway, B. Dunham, R. Eichhorn, C. Gulliford, V. Kostroun, C. Mayes, K. Smolenski, N. Taylor, Xelera Research LLC, Ithaca, NY, USA  
 W. Bergan, D. Kayran, E. Wang, D. Xu, Brookhaven National Lab, Upton, NY, USA  
 N. Wang, Cornell University, Ithaca, NY, USA

## Abstract

Microbunched electron Cooling (MBEC), a type of Coherent electron Cooling (CeC), is a possible way to cool high energy protons; such an electron cooler can be driven by an energy recovery linac (ERL). The beam parameters of this design are based on cooling 275 and 100 GeV protons at the Electron-Ion Collider (EIC), requiring 150 and 55 MeV electrons, respectively. If implemented, a high energy cooler would serve to increase the average luminosity of the collider by mitigating the emittance growth caused by various processes. This ERL is designed to deliver a bunch charge of 1 nC, an average current of 100 mA, and strict requirements on the transverse emittance, slice energy spread, and longitudinal distribution profile. This paper covers the current state of the design.

## INTRODUCTION

The Electron-Ion Collider (EIC) is a partnership project between Brookhaven National Lab (BNL) and Thomas Jefferson National Accelerator Facility (TJNAF) to be constructed at BNL, using much of the existing infrastructure of the Relativistic Heavy Ion Collider (RHIC). Collisions occur between the hadrons in the Hadron Storage Ring (HSR) and the electrons supplied by the Electron Storage Ring (ESR); in order to maintain a high average polarization of the ESR, bunches are frequently replaced using the Rapid Cycling Synchrotron (RCS). While most of the magnets for the HSR are repurposed RHIC magnets, already installed in the existing tunnel, both the ESR and RCS will have to be installed. In the current scope of the EIC, only one interaction region (IR) is supported, sited at the current IR6 of RHIC; however, it is highly desired that a second IR may be supported at IR8 in the future, and design efforts support that eventuality [1].

The present EIC baseline only includes cooling of the injected hadron beam prior to ramping. However, it is possible that a future upgrade to improve the luminosity will be desired, requiring the hadron bunches to be cooled during collision in order to maintain the beam emittance [2].

## ERL DRIVEN COOLER

The ERL design presented here is intended to cool a high energy hadron beam with microbunched electron cooling; the lattice is presented with the optics suitable for the EIC

275 and 100 GeV protons, which requires 150 and 55 MeV electrons, respectively. The necessary beam parameters for both energies are given in Table 1; for an explanation of the development of these parameters, please see [3]. Given the significant beam power necessary, it is clear that an energy recovery linac (ERL) is required - the operational power to produce the same beam parameters with a linac is prohibitive; additionally, using an ERL reduces the radiation considerations at the beam dump. Closed optics exist for both operational modes, shown in Fig. 1.

Table 1: The electron beam parameters for the two proton beam energies. The electron beam longitudinal distribution is assumed to be a supergaussian of order ~4.

Proton Energy	100 GeV	275 GeV
Gamma	107.6	294
Energy (MeV)	55	150
Bunch charge (nC)		1
Rep. rate (MHz)		98.5
Avg. current (mA)		98.5
rms bunch length (mm)	9	7
Peak current (A)	10	13
Slice energy spread $dp/p(10^{-4})$	0.6–1.5	0.4–0.8
Norm. trans. emit. (mm-mrad)		2.8

## LAYOUT

A representative layout of the ERL is shown in Fig. 2. In beamline order during energy recovery, the sections are the injector, the merger, the booster, the bunch compressor and high energy bypass lines (PX), the main linac, the beam dump, the laser heater, transport to the cooling section, the cooling section (modulator, amplifier, and kicker), the first turnaround, the return line, and the second turnaround – after which, the beam begins energy recovery. Alternatively, the beam can be steered through the merger into the diagnostic line.

The injector consists of a photocathode DC gun and a cryomodule containing three superconducting radio frequency (SRF) cavities – two 197 MHz quarter-wave resonators (QWRs) and a 591 MHz single-cell cavity. The beam is

\* kirstend@jlab.org

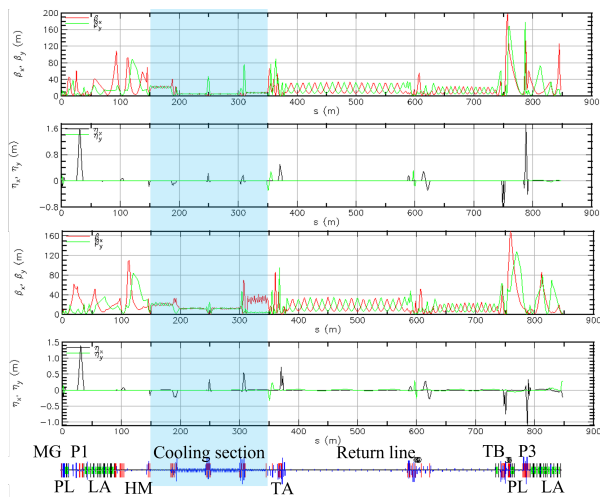


Figure 1: The preliminary designs of the 150 and 55 MeV electron coolers. Shown are the beta functions in meters (top) and dispersion in meters (bottom), all as a function of  $s$  in meters, with the upper and lower pair corresponding to the 150 MeV and 55 MeV design, respectively. Below the four plots is the component layout, with the various sections labeled.

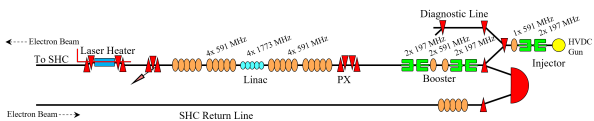


Figure 2: Represented is the injector, followed by the merger, going to either the diagnostic line or the booster, the bunch compressor and high energy bypass lines (PX), the main linac (Linac), the dump chicane, the laser heater, the transport to the cooling section, and the return line from the cooler, after which the beam energy recovers and is steered into the dump line.

accelerated to roughly 6 MeV and the accelerating cavities are run off-crest so that the bunch is chirped to allow for bunch compression later; the single cell cavity is at the third harmonic of the 197 MHz frequency and is used to linearize the longitudinal phase space.

The booster consists of two cryomodules, oriented so that the cavity order is two 197 MHz QWRs, two 591 MHz, and two 197 MHz QWRs. The beam energy is roughly 13 MeV, the bunch is significantly chirped, and the single cell cavities are again used to linearize the longitudinal phase space; however, the longitudinal phase space is evaluated after the bunch compressor in the following section.

Next, the beam enters the PX section, shown in Fig. 3, which consists of the P1, P2, and P3 lines. Each line is energy-specific and during the acceleration of both configurations, the 13 MeV beam goes down the P1 line, which compresses the bunch; bunch compression is tunable due to the quadrupole magnets included in the compressor. A more in-depth description is in a later section.

Following the PX section is the main linac, consisting of eight 591 MHz five-cell SRF cavities and four 1773 MHz five-cell SRF cavities, with the 1773 MHz cavities placed in the center and four 591 MHz cavities on either side. The beam is accelerated to the top energy of either 150 or 55 MeV and is no longer chirped. Similar to the injector and booster, the longitudinal phase space is linearized with the 1773 MHz cavities.

The dump chicane and the laser heater chicane follow the main linac, after which the beam is transported to the cooling section, which consists of the modulator, amplifier, and kicker. After the cooling section, the beam separates from the HSR before entering a Bates bend and going down the return line.

At the end of the return line is a 591 MHz five-cell SRF cavity, which is run at the zero crossing and chirps the beam, minimizing the energy spread of the beam at the dump. Without this chirp cavity, the only way to minimize the energy spread is to have the beam energy at the dump to be significantly different than the 6 MeV injection energy.

After the return line is a second Bates bend – following this, the high energy line merges with the injection line, and the chirped beam begins deceleration and energy recovery. The beam is decelerated during the second pass through the booster, then enters the PX section. For the second pass through PX, the beam enters either the P2 or P3 beamline, corresponding to the 55 and 150 MeV modes, respectively. During the second pass through the linac, the beam decelerates to the injection energy and is transported to the beam dump.

## TIME OF FLIGHT CONSIDERATIONS

Typically, ERLs have a single linac and consequently, only a single time of flight concern – the time of flight between the linac exit and the linac entrance. However, this machine has two accelerating sections, the booster and the linac, which means that there are two time of flight concerns. The first concern is the time of flight between the booster exit and the booster entrance; the second is the time of flight between the linac exit and the linac entrance.

The booster time of flight uses path length changes in the two Bates bends for flexibility, similar to the Jefferson Lab Free Electron Laser ERL drivers; correctors at the entrance and exit of the Bates bend allow for the beam to enter and exit on-axis, while the beam orbit through the magnet is off-axis, changing the path length through the Bates bend [4]. At the 197 MHz fundamental frequency of the booster and a 2.5 cm maximum orbit excursion at the center of the bend, this translates to a range of  $\pm 11.7^\circ$  per Bates bend. However, the length of this machine introduces a complication – for a fixed path length on the order of 800 m, the time of flight for the two energies differs by roughly  $8^\circ$  at the booster frequency, but the time of flight between the booster exit and entrance is required to be the same for both modes. The second Bates bend was placed so that the relevant time of flight was roughly  $4^\circ$  from the requirement for both energies

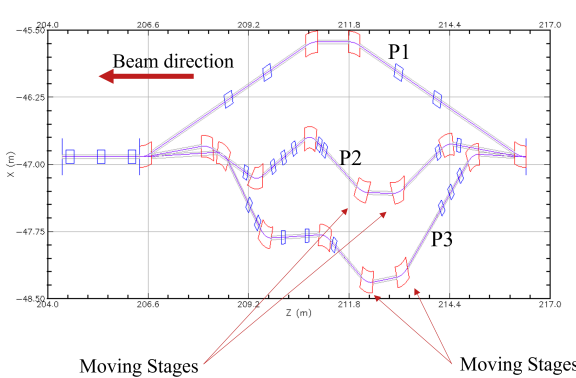


Figure 3: The floor layout of the PX section; the three separate lines are P1, P2, and P3, top to bottom (as labeled), which correspond to the beam energies of 13, 48, and 143 MeV, respectively. The “common” dipoles are the right most and left most dipoles, which is a common magnet for all three beam energies. In both the P2 and P3 lines, the second and third dipoles are on moving stages which can be remotely controlled to change the physical path length of the on-axis orbit.

and by design, both energies travel through the second Bates bend off-axis to achieve the requisite time of flight.

The linac time of flight is controlled by the path length through the appropriate high energy PX line. Both P2 and P3 have moving stages in order to physically move two dipoles and change the on-axis path length through the lines, similar to the moving stages in the CBETA splitters [5, 6].

## PX SECTION

The floor plan of the PX section, with the separate lines labeled, is shown in Fig. 3. The design of this section allows for the ERL to switch operational modes without requiring a change to the physical layout of the machine.

Each line in PX corresponds to a specific beam energy; P1, P2, and P3 are designed for beam energies of 13, 48, and 143 MeV, respectively. P1 compresses the accelerating beam for both modes, while P2 and P3 transport the decelerating beams for the top energies of 55 and 150 MeV, respectively. While all lines are achromats, none is isochronous; though it would be ideal for  $R_{56}$  to be zero in P2 and P3, it is more critical to close dispersion, dispersion prime, and control the transverse optics through these lines. Given that the decelerating beam is chirped, the non-zero  $R_{56}$  of these lines does mean that some bunch stretching occurs. If necessary, the  $R_{56}$  of the second Bates bend can be tuned to compress the bunch, so that the bunch length during the second pass the linac is sufficiently short.

In order for the time of flight requirement between the linac exit and entrance to be correct, the booster time of flight must be correct. This is driven by the limited range of the moving stages, i.e., the limited time of flight flexibility in the P2 and P3 lines, as well as the inherent geometry of the PX section; if the decelerating beam enters either

high energy line at an energy significantly different than design, the beam will be lost on the beam pipe wall before reaching the first high energy dipole. While the 150 and 55 MeV configurations have very similar linac time of flight requirements, the P3 line has an extra wavelength of path length in order to remove geometry conflicts with the P2 line. As the two lines have different geometries, the time of flight flexibility is different. The P2 line has a range of  $\pm 35^\circ$ , while the P3 line has a range of  $\pm 55^\circ$ , both with respect to the 591 MHz fundamental frequency of the linac.

The design before the main linac, particularly the booster and PX sections, is motivated by the need to produce a supergaussian longitudinal distribution, with small slice energy spread and transverse emittance. At present, we achieve this by producing a very long bunch at the gun, which controls both the slice energy spread and transverse emittance, until the beam is at a sufficiently high energy that when the bunch is compressed to the requisite bunch length, these parameters are relatively unperturbed through the compression process.

The inclusion of a bunch compressor within the accelerating section of an ERL is not a typical configuration, and its inclusion makes the design more complex. As a design alternative, the injector energy could be increased to 13 MeV and the bunch compressed before the merger. This would have the benefit of returning to a more simple ERL layout, with a single time of flight requirement and no need for higher-energy bypass lines to transport the decelerating beam around the compressor chicane. However, this design comes with other drawbacks – lower energy efficiency and higher shielding requirements at both the dump and the diagnostics line. Another alternative is to compress the 6 MeV bunch in the injector – however, this approach does not produce the required beam parameters.

## CONCLUSION

We have developed a conceptual design for both energy modes of an ERL-driven cooler, which is capable of cooling high energy protons during collisions at the EIC. One critical success of this design is that the magnet layout is unchanged between configurations, so no vault access is required between switching energies. Though more complex than many ERLs, no show stoppers have been found. While it may be more feasible for the EIC parameters to consider a different cooling mechanism, this ERL design’s ability to produce a high-charge, high-brightness electron beam makes it a good design starting point for future high energy cooling considerations.

## ACKNOWLEDGMENTS

This work is supported by Jefferson Science Associates, LLC under U.S. DOE Contract DE-AC05-06OR23177 and Brookhaven Science Associates, LLC, Contract DE-SC0012704, while Xelera was supported by the U.S. DOE Small Business Innovation Research (SBIR) Phase II program under Federal Grant Number DE-SC0020514 during earlier stages of this work.

## REFERENCES

- [1] C. Montag *et al.*, “The EIC accelerator: design highlights and project status”, in *Proc. IPAC’24*, Nashville, TN, May 2024, pp. 214-217. doi:[10.18429/JACoW-IPAC2024-MOPC67](https://doi.org/10.18429/JACoW-IPAC2024-MOPC67)
- [2] K. Deitrick *et al.*, “Development of an ERL for coherent electron cooling at the Electron-Ion Collider”, in *Proc. IPAC’24*, Nashville, TN, May 2024, pp. 3086-3089. doi:[10.18429/JACoW-IPAC2024-THPC40](https://doi.org/10.18429/JACoW-IPAC2024-THPC40)
- [3] W. Bergan *et al.*, “Coherent electron cooling physics for the EIC”, in *Proc. IPAC’24*, Nashville, TN, May 2024, pp. 2937-2942. doi:[10.18429/JACoW-IPAC2024-THYD1](https://doi.org/10.18429/JACoW-IPAC2024-THYD1)
- [4] D. Douglas, “Some features of the FEL upgrade  $\pi$ -bends”, Rep. JLAB-TN-01-024, May 2001.
- [5] G. H. Hoffstaetter *et al.*, “CBETA design report, Cornell-BNL ERL test accelerator”, 2017, arXiv:1706.04245 [physics.acc-ph]. doi:[10.48550/arXiv.1706.04245](https://doi.org/10.48550/arXiv.1706.04245)
- [6] A. Bartnik *et al.*, “CBETA: first multipass superconducting linear accelerator with energy recovery”, *Phys. Rev. Lett.*, vol. 125, p. 044803, 2020. doi:[10.1103/physrevlett.125.044803](https://doi.org/10.1103/physrevlett.125.044803)